

# Tensile Properties of Elastomeric Polyolefin Thin Films: The Path to Failure

SARAH T. ECKERSLEY, A. BRUCE CHAPUT

The Dow Chemical Company, Emulsion Polymers, 1604 Building, Midland, Michigan 48674

Received 14 September 1999; accepted 1 July 2000

**ABSTRACT:** The tensile failure of thin films prepared from polyolefin elastomer dispersions was studied. The elastomer dispersions were composed of copolymers of ethylene and 1-octene, dispersed in water at solids concentrations of approximately 50%. The density of the polyolefin resins ranged from 0.855 to 0.885 g cm<sup>-3</sup>. The melt index of the resins ranged between 0.5 and 5.0 g 10 min<sup>-1</sup>. As expected, the tensile strength of neat polyolefin films was found to be a strong function of the density and a weak function of the melt index. Dispersion blends were prepared from neat polyolefin dispersions. The film tensile properties were measured as a function of the blend ratio and the particle-size ratio. The blend ratio was found to be the dominant factor. It was found that blending the dispersions had an antagonistic effect on the tensile properties. The ultimate tensile strength of the blend film was lower than expected from the arithmetic mean behavior (based on the weight fraction) of the two constituent resins. A similar result was observed for the ultimate elongation, that is, blending of the two elastomers gave inferior behavior. The relationship between the experimental tensile properties and the blend ratio fit a quadratic function. A Monte Carlo simulation was used to model film failure in two dimensions. The two particle types were assumed to pack randomly and failure was forced to occur by the lowest-energy path. The simulated ultimate tensile strength was also found to be a quadratic function of the blend ratio, confirming the suitability of the model. © 2001 John Wiley & Sons, Inc. *J Appl Polym Sci* 80: 2545–2557, 2001

**Key words:** dispersion; polyolefin; elastomer; tensile; blend; Monte Carlo simulation

## INTRODUCTION

Blending is a common approach to enhance the performance of materials. In most cases, the intent is to deliver the best features of each individual component to provide enhanced performance. Many applications utilize latex blends in this manner, but much of the blend literature for latexes is related to coatings applications.<sup>1–3</sup> The research reported here was concerned with blends of elastomeric latexes for use in thin-film applica-

tions. Familiar examples of thin-film applications include balloons, disposable gloves, and condoms. Our research investigated the effect of the film morphology on the tensile behavior of thin films prepared from blends of elastomeric latexes. The tensile behavior was studied experimentally and simple Monte Carlo simulations were used to model the behavior.

The elastomer dispersions studied here are experimental polyolefin dispersions. These differ from conventional emulsion, dispersion, or suspension polymers which are produced by free-radical processes. Rather, polyolefin dispersions are prepared directly from solid polyolefin elastomer resin. In particular, our research focused

---

Correspondence to: S. T. Eckersley.

*Journal of Applied Polymer Science*, Vol. 80, 2545–2557 (2001)  
© 2001 John Wiley & Sons, Inc.

on polyolefin dispersions produced from copolymers of ethylene and  $\alpha$ -olefins. Constrained geometry catalysts allow the incorporation of high levels of  $\alpha$ -olefin, yielding elastomeric materials. These polyolefin dispersions are unconventional elastomers, in that they are thermoplastic semicrystalline elastomers prepared as water-based dispersions. However, it is hoped that the results of this work can be extended to blends of more conventional elastomers and to other latex blend systems.

## BACKGROUND

Thin free film applications typically require a combination of high tensile strength and high elongation at failure, combined with softness (or low stress at low elongation). Sulfur-vulcanized natural rubber latex has an advantageous combination of strength, softness, and elasticity. Unfortunately, natural rubber contains a protein that produces a severe allergic reaction in a significant percentage of the population.<sup>4,5</sup> This is a serious, growing concern associated with the use of natural rubber which is motivating the search for alternatives. Several alternative elastomers and thermoplastics are currently used in thin-film applications. These include nitrile rubber, polyurethanes, and PVC plastisol. Polyolefins are a relatively new development in the elastomer field which may have utility in thin-film applications.

### Polyolefin Technology

Polyolefin resins are produced using single-site-constrained geometry catalysts. This catalyst technology allows the design and production of copolymers not previously accessible with conventional Ziegler–Natta-type catalysts.<sup>6</sup> Copolymers of ethylene and aliphatic  $\alpha$ -olefins can be produced with high levels of the  $\alpha$ -olefin comonomer, narrow molecular weight distributions, and uniform polymer structure.<sup>7</sup> In the case of the copolymers discussed here, 1-octene is the comonomer employed. Copolymerization with 1-octene yields hexyl branches along the main chain. The hexyl branches disrupt crystallization, which yields very low density semicrystalline resins with unique physical properties.

Ethylene–octene copolymers are thermoplastic elastomers, which have tie chains that link the crystalline domains. An illustration of the polymer morphology is shown in Figure 1. The resin

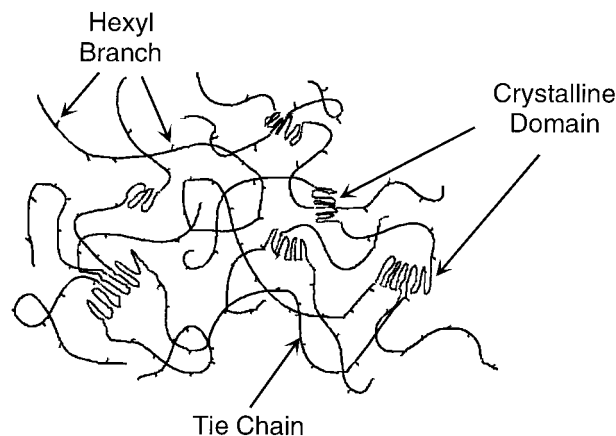


**Figure 1** Polyolefin semicrystalline microstructure schematic.

physical properties are related to the crystallinity (expressed in terms of the density), the molecular weight (expressed in terms of the melt index), the molecular weight distribution, degree of long-chain branching, and comonomer homogeneity. Semicrystalline polymers display two thermal transitions. The glass transition temperature ( $T_g$ ) of ethylene–octene copolymers is approximately  $-45^\circ\text{C}$  (and can be as low as  $-70^\circ\text{C}$ , depending on the density). The exceptional low-temperature flexibility of polyolefins is due to the very low  $T_g$ . A second thermal transition occurs at higher temperature. This melting transition is dependent on the degree of crystallinity of the particular polyolefin. For the polyolefin dispersion resins, melting temperatures range between approximately  $40$  and  $90^\circ\text{C}$ , for resins ranging in density from  $0.855$  to  $0.890\text{ g cm}^{-3}$ . The crystallinity and molecular weight also determine the tensile properties, as will be shown later.

### Blend Technology

Latex blends represent a unique technology for combining the properties of the constituent components. Previous research in this laboratory focused on the relationship between the blend film performance and the morphology in coating systems.<sup>1</sup> These studies showed that mass ratios of the two components, as well as the particle-size ratio, impact the film morphology and performance. These effects are related to the packing of the two particle types and can be explained in terms of the percolation theory.<sup>8–10</sup> Figure 2 illustrates that the effect of these parameters is directly related to particle packing. Figure 2 shows

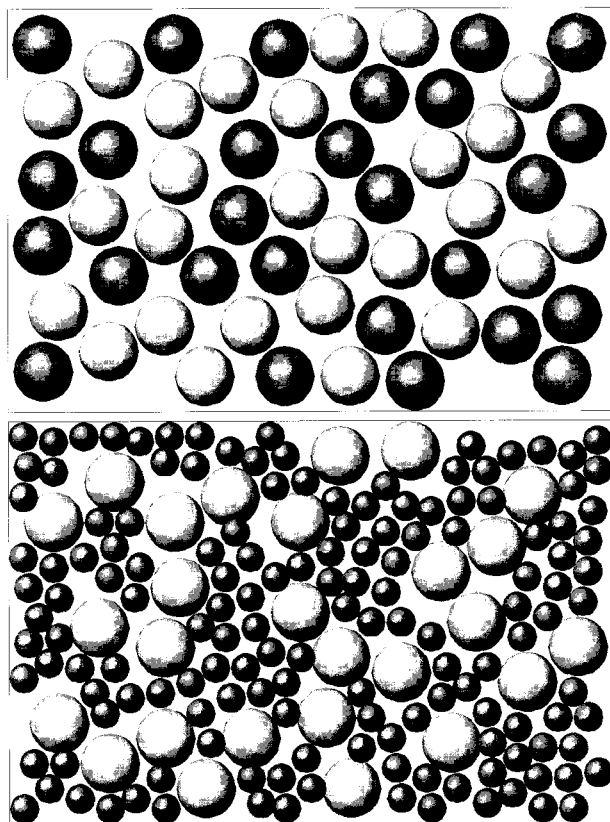


**Figure 2** Illustration of particle packing for two particle-size ratios.

two latex blends where the two components (light and dark spheres) are present in equal concentration. In the upper illustration, the particle sizes are equal. The particles pack randomly and neither phase is continuous. In the lower illustration, the dark particle diameter is half that of the light particles. In this case, the dark particles form the continuous phase. The composition of the continuous phase is determined by both the mass ratio and the particle-size ratio.

## EXPERIMENTAL

### Latex Preparation

Polyolefin dispersions were prepared using the dispersion process described previously.<sup>11</sup> A simplified flow sheet of the process used to obtain polyolefin dispersions is shown in Figure 3. The polymer and an appropriate solvent are added to a jacketed vessel, heated, and mixed to form a uniform polymer solution. Often, the surfactants required to make the dispersion are dissolved in

this solution. Alternatively, the surfactant may be supplied in the aqueous feed for the dispersion, which is stored in a separate feed tank. This is the configuration depicted in Figure 3. A number of surfactants can be used to prepare the dispersions. Common anionic surfactants at concentrations of 2–5% (based on the polymer) are typical. The polymer and aqueous solutions are fed to a disperser unit, which provides the shear required to generate the dispersion.

The dispersion leaving the disperser is water-continuous and extremely viscous. Usually, dilution water is added to reduce the viscosity and to improve the dispersion stability. The diluted dispersion is then transferred to a stripper vessel, where the solvent is removed by steam distillation or vacuum-evaporation. The resulting polyolefin dispersion is normally concentrated to approximately 50% solids by evaporating the excess water. The overhead vapor stream from the stripper vessel is condensed, and the water and solvent streams are recycled to the process.

The resins used to make the dispersions were obtained from The Dow Chemical Co. and DuPont Dow Elastomers and were used as provided. AFFINITY\* plastomers are available from The Dow Chemical Co. and ENGAGE† elastomers are available from DuPont Dow Elastomers. The resin characteristics (density and melt index) were provided to the authors. The melt index was

\*Trademark of The Dow Chemical Co., Midland, MI.

†Trademark of DuPont Dow Elastomers L.L.C., Wilmington, DE.

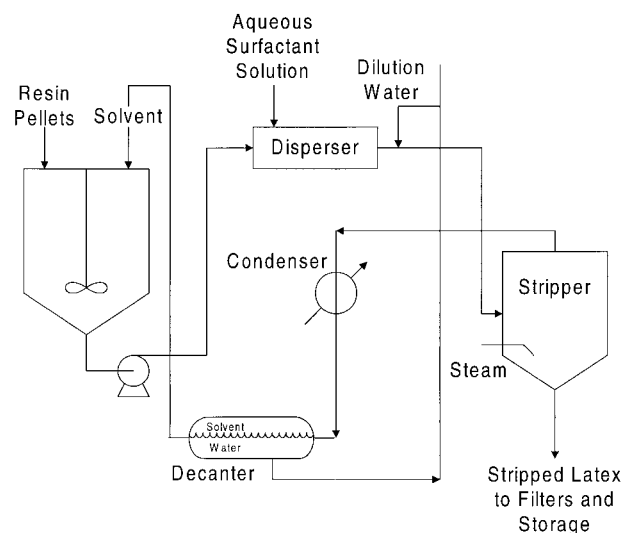


**Figure 3** Simplified lab emulsification diagram.

**Table I** Latexes for Particle-size Blends

Latex	C, Small	A, Large	C, Intermediate	A, Intermediate	C, Large	A, Small
Particle diameter ( $\mu\text{m}$ )	0.5	1.6	1.0	1.0	1.7	0.7
Ratio, $D_{\text{Resin C}}/D_{\text{Resin A}}$		0.3		1.0		2.5

determined using a 2.16-kg weight, at a temperature of 190°C.

### Differential Scanning Calorimetry

Melting temperatures were obtained by differential scanning calorimetry (DSC) using a TA Instruments Dual Cell DSC-2100 equipped with a mechanical cooling accessory. Approximately 20 mg of each polymer was heated to 120°C and held for 1 min, cooled, and then immediately scanned from -20 to 120°C at 10°C min<sup>-1</sup>. The (inverted) peak of the broad melting endotherm was chosen as the temperature of maximum melting.

### Particle-size Analysis

The particle-size distribution of each dispersion was determined using a Coulter LS230 particle-size analyzer. This device measures particles ranging in size from 0.04 to 2000  $\mu\text{m}$ . Particle-size information for the dispersions used in this study is found in Table I.

### Tensile Testing

Free films about 6 mil thick were prepared by a drawdown method on preheated glass plates. The film was dried in a humidity-controlled environment for about 30 min. The temperature and relative humidity (RH) were varied according to the conditions required for a particular resin. Typical conditions were 80°C and 50% RH. Modified ASTM test procedures designed for elastomers were employed.<sup>12</sup> Tensile properties (ultimate tensile strength, ultimate elongation, and modulus) were measured on an Instron Model 4501 tensile tester, using a crosshead speed of 20 in min<sup>-1</sup>. Typically, between 10 and 15 specimens were tested.

## RESULTS AND DISCUSSION

Three types of polyolefin dispersions were prepared. Single-component dispersions were made from single resins. Dispersion blends were pre-

pared by blending two distinct polyolefin dispersions, having equal and unequal particle sizes. Finally, a "resin blend" was prepared by blending the resin pellets prior to emulsification.

### Film Formation from Polyolefin Dispersions

Full development of the tensile properties in a film prepared from an emulsion polymer is contingent on adequate film formation. The film-forming behavior of polyolefin dispersions differs from that of conventional emulsion polymers. Film formation of conventional emulsion polymers is frequently characterized by the minimum film temperature (MFT). At temperatures below the MFT, the latex dries to form a powder. At temperatures above the MFT, a continuous polymer film is formed. The MFT is related to viscoelastic properties in the case of an amorphous emulsion polymer, as well as other polymer and latex characteristics.<sup>13</sup> For a conventional emulsion polymer, the MFT is closely related to the polymer glass transition temperature ( $T_g$ ).

In the case of polyolefin dispersions, coalescence is controlled by the melting transition, which, in turn, is controlled by the crystallinity. Semicrystalline polymers do not have a single melting temperature, but rather a distribution of melting temperatures. Figure 4 shows the melting temperature ( $T_{\text{mp}}$ ) as a function of density, as determined by differential scanning calorimetry (DSC) for films prepared from polyolefin dispersions. The melting point is assigned to be the maximum temperature in the melting endotherm. For  $T \ll T_{\text{mp}}$ , a polyolefin dispersion dries to form a powder. Drying at  $T < T_{\text{mp}}$  yields a film with low cohesive strength. When the dispersion is dried at  $T \geq T_{\text{mp}}$ , the resultant film has tensile properties equivalent to those of the precursor resin.

Polyolefin dispersion blends are bimodal blends of polymers with distinct tensile properties. It is assumed that during blend film formation coalescence of the particles occurs to the degree that the film is continuous, yet discrete do-

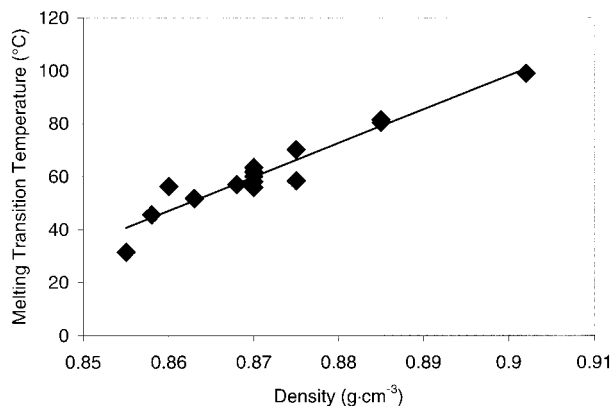


**Figure 4** Melting transition as a function of polyolefin resin density.

mains of the two resins remain. This is a reasonable assumption, since film formation occurs at a temperature just slightly above the melt transition. The degree of interdiffusion is sufficient to yield a coherent film. However, it is unlikely that large-scale interdiffusion will occur, since the molten resin is highly viscous. The residual domains will correspond to the precursor dispersion particles. Tensile failure of such a film will depend on the film morphology, as well as on the tensile properties of the constituent polymers.

### Single-component Dispersions

The film properties of neat polyolefin films are related to the resin density and melt index. The density varies with the crystallinity of the polymer, which is determined by the fraction of  $\alpha$ -olefin comonomer incorporated into the polymer during polymerization. The density and crystallinity decrease with increasing  $\alpha$ -olefin content. The melt index is commonly used for polyolefin resins and is inversely correlated with the molecular weight. The tensile properties of the neat resins were measured. The resin characteristics are listed in Table II. The resins are all copolymers of ethylene and 1-octene, which differ primarily in terms of 1-octene content and molecular weight.

The stress/strain behavior of polyolefin dispersion film prepared from resins A and D is shown in Figure 5. The curves are characteristic of elastomers. The stress/strain behavior of a vulcanized natural rubber latex film is shown for comparison. Not surprisingly, it also exhibits elastomeric behavior. The main difference between the vulcanized rubber and the polyolefin is seen at low strain. In the case of the vulcanized rubber, the

stress at low strain is much lower than for the polyolefin. It is this low stress at low elongation that gives vulcanized natural rubber its characteristic softness in thin films.

Thin-film tensile data are given in Table III. The data are reported as the mean  $\pm$  95% confidence limit. The first three sets of data presented in Table II (resins A, B, C) show the effect of density on the film properties for a fixed melt index (0.5 g/10 min). The tensile strength increases with increasing density (or crystallinity), while the elongation at break decreases. The stress at low (200%) elongation increases with increasing density. Comparison of the data sets for resin C and resin D shows the effect of the melt index on the physical properties for a fixed density (0.870 g cm<sup>-3</sup>). The tensile strength is independent of the melt index (within experimental error) for the range of melt index studied here. For a broader range of the melt index, it would be expected that the tensile strength would decrease with an increasing melt index. The data indicate that the degree of crystallinity is the most important parameter influencing the tensile strength for the melt index range studied. The data also show that the higher melt index polymer gives a softer film, with a higher elongation at break. The tensile strength and film softness are in opposition. This is expected, but contrary to the desired situation for thin-film applications. It was hypothesized that a blend approach would yield optimized performance intermediate between two individual resins.

### Blend-ratio Effect

Resin A had the lowest stress at 200% elongation, but, correspondingly, low tensile strength. It was decided to determine if the tensile strength of A could be increased via blending while maintain-

**Table II** Characteristics of Ethylene-Octene Copolymers Used in Preparation of Single-component Dispersions

Resin	Density (g cm <sup>3</sup> )	Melt Index (g 10 min <sup>-1</sup> )
A	0.855	0.5
B	0.863	0.5
C	0.870	0.5
D	0.870	5
E	0.885	1

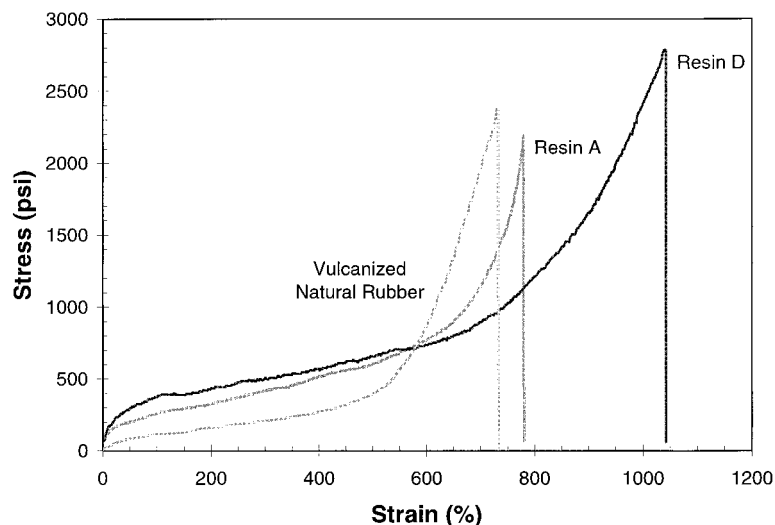


Figure 5 Tensile behavior of polyolefin and vulcanized natural rubber films.

ing the other desirable properties, such as softness. The following blend pairs were evaluated: Resin E/Resin A and Resin D/Resin A.

The effect of the blend ratio on the tensile strength for Resin E/Resin A is shown in Figure 6. The mean is shown, along with an error bar representing the 95% confidence interval. The experimental data were fitted to a second-order polynomial with an  $R^2$  value of 0.993. A line representing the arithmetic mean is also shown in Figure 6. It is evident from Figure 6 that the relationship between the tensile strength and the blend ratio is not a simple average. The tensile strength is lower than is the weighted average, suggesting that failure occurs in weaker domains of the film. At very low concentrations of the weaker (lower crystallinity) Resin A polymer, the Resin A domains are small (of the order of a single-particle diameter) and discrete. A substantially lower-energy pathway is achieved when failure occurs through these domains. Therefore, the tensile strength is strongly dependent on the

Resin A concentration. At very high concentrations of Resin A, the weaker polymer forms the continuous phase, providing a continuous low-energy pathway for film failure. Therefore, at high concentrations of the weak polymer, the tensile strength is nearly independent of the presence of inclusions of a stronger material.

A distinct trend is not apparent in the ultimate elongation data. However, it is clear the elongation of the blends is less than is the weighted average of the constituent polymers. The stress at 200% elongation is clearly linearly dependent on the mass ratio, with the line of best fit shown. This indicates that at low elongation the stress is averaged over the entire specimen.

#### Particle-size Effect

In previous research,<sup>1</sup> it was shown that the film morphology had an effect on the performance properties in coatings applications. It was hypothesized that an analogous effect would be observed

Table III Tensile Properties of Thin Films Prepared from Single-component Dispersions

Resin	Density (g cm <sup>3</sup> )	Melt Index (g 10 min <sup>-1</sup> )	Ultimate Tensile Strength (psi)	Ultimate Elongation (%)	Stress at 200% Elongation (psi)
A	0.855	0.5	1200 ± 160	1040 ± 30	195 ± 4
B	0.863	0.5	2120 ± 180	831 ± 44	311 ± 5
C	0.870	0.5	2625 ± 70	650 ± 10	480 ± 20
D	0.870	5	2590 ± 40	1030 ± 40	310 ± 70
E	0.885	1	5040 ± 280	665 ± 6	850 ± 40

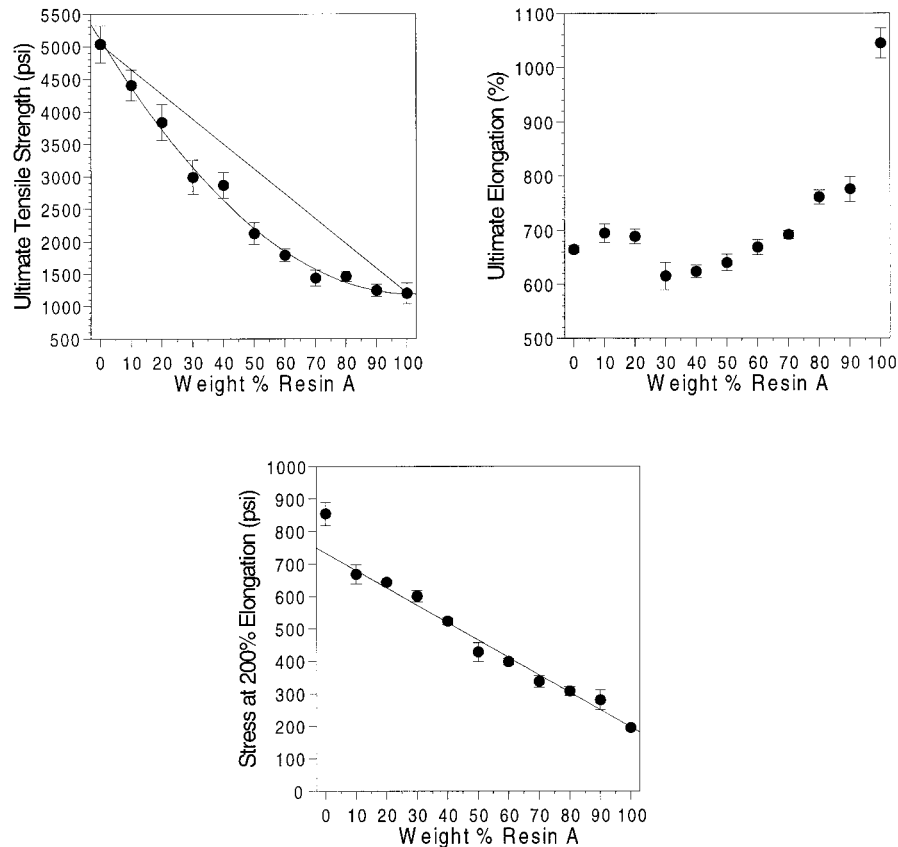


**Figure 6** Tensile properties as a function of blend ratio for blends of Resin A and Resin E ( $D_{\text{Resin E}}/D_{\text{Resin A}} = 1.0$ ).

for the tensile behavior of the polyolefin dispersion blend films. The film morphology is affected by the relative particle sizes of the constituent latexes, as illustrated by the schematic of Figure 2. The effect of the particle-size ratio on the tensile properties was investigated for blends of Resin A and Resin C. The particle-size ratio is expressed in terms of the ratio of the diameter of the Resin C latex to the Resin A latex (i.e.,  $D_{\text{Resin C}}/D_{\text{Resin A}}$ ). Three particle-size ratios were investigated: 0.3, 1.0, and 2.5. The variation in the particle-size ratio was accomplished by varying the diameters of both of the constituent latexes and is described in Table I.

Figure 7 shows the ultimate tensile strength as a function of the blend ratio and the particle-size ratio. The tensile strength of a resin blend is also shown for comparison purposes. There are several important features revealed by the data shown in Figure 7. The high degree of uncertainty in the tensile measurements is apparent. For example, the tensile strength of a fully annealed film of neat polyolefin latex should be constant, regard-

less of the particle size of the precursor latex. The 0% Resin A data for the three data sets varied between 2250 and 2700 psi. This is the result of several factors: Tensile failure tends to be initiated at flaws or inclusions in the film, which introduces variability. However, the data are illuminating, despite the high degree of variability.

In general, the data follow a second-order polynomial functional form. The introduction of low-strength domains into the high-strength matrix has a pronounced effect on the tensile strength. As the concentration of low-strength material is increased, the effect is diminished. This is consistent with the low-strength material forming the continuous phase, which fails preferentially. Not surprisingly, a similar trend is seen in the elongation data, with the ultimate elongation corresponding to the material which forms the continuous phase. The 200% modulus follows a linear relationship, rather than the polynomial form, presumably because the film is not being stressed to failure at that elongation.

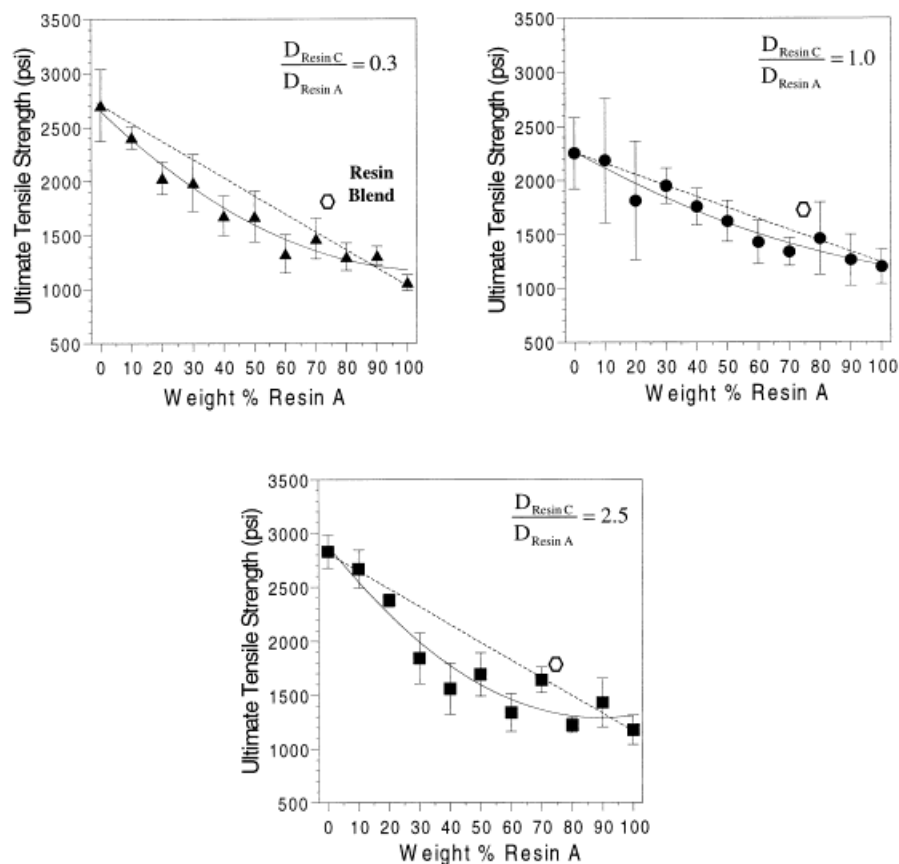


**Figure 7** Tensile strength as a function of blend ratio for blends of Resin A and Resin C.

The tensile data shown in Figures 7–9 indicate that there is no performance advantage to be gained from blending dispersions. For example, the tensile strength of Resin A is increased slightly (from  $\sim 1200$  to  $1500$  psi) by blending with 40% Resin C. However, the elongation is decreased from  $\sim 1000$  to  $750\%$  and the modulus is increased from  $\sim 210$  to  $320$  psi. These properties are inferior to neat Resin B. The resulting blend is weaker and equivalently stiff, compared to Resin B. The tensile strength of the blend systems are also inferior to the resin blend (75 wt % A, 25 wt % B), which was prepared by blending the two polyolefins at the molecular level during the emulsification process. The elongation of the blend film was also lower than would be expected based on the weighted-average elongation of the constituent latexes. However, there is not a discernible difference between the elongation of the blend film and the resin blend film. There is no obvious explanation, save experimental error.

It was hypothesized that the particle-size ratio would have an effect on the tensile properties. A

clear trend is not apparent in the data of Figures 7–9. There is sufficient error in the data to mask any subtleties, should they exist. It is clear, however, that the film morphology due to blending has an effect on the tensile properties. In an effort to better understand the effect of the film morphology on the tensile behavior, film tearing was modeled using a Monte Carlo simulation of a blend composed of two elastomers occupying discrete domains.

#### Failure of Polyolefin Dispersion Blends: Monte Carlo Simulation

Monte Carlo simulation is a useful tool when a complex system can be represented as a set of simpler systems for which known behaviors exist. Fracture mechanics fit this criteria since the gross phenomena of failure of the complex system can often be broken into a simpler set of individual failures and load distributions. To this end, Monte Carlo simulations have found use in the simulation of stress corrosion cracking,<sup>14</sup> fiber-



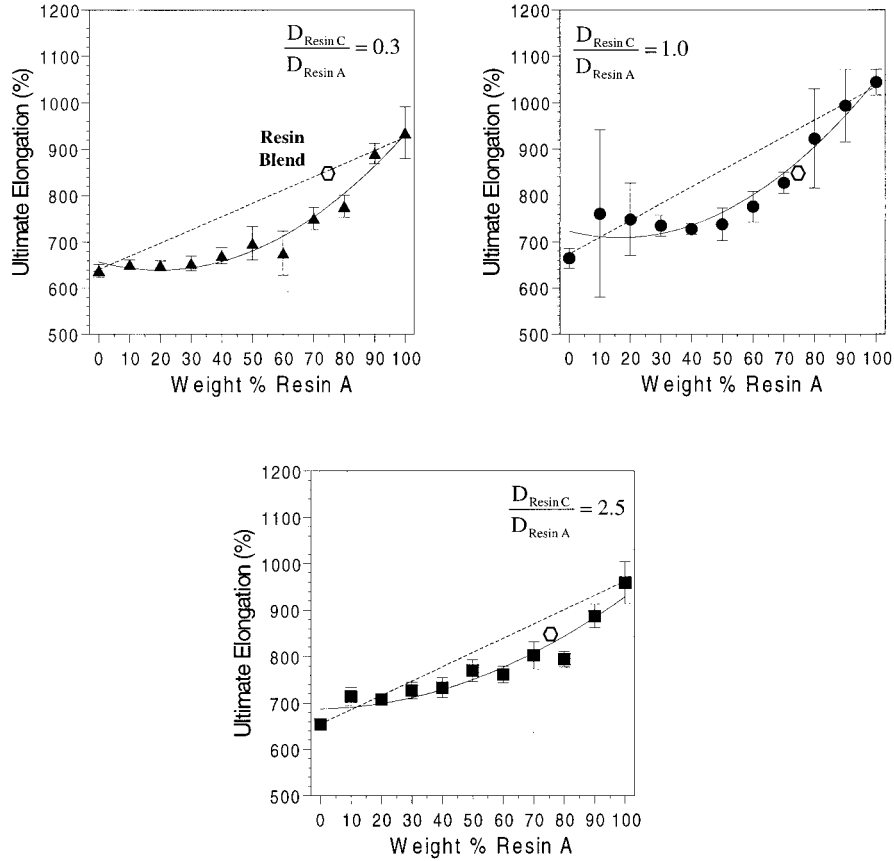


**Figure 8** Ultimate elongation as a function of blend ratio for blends of Resin A and Resin C.

filled composite failure,<sup>15</sup> fracture of rock,<sup>16</sup> and fatigue of superalloys.<sup>17</sup> Polyolefin dispersion blend films are assumed to be composed of discrete domains with known tensile properties. Therefore, Monte Carlo simulations may be applicable to these systems.

A simplifying assumption can be made that tensile failure of a blend film will occur by the pathway with the lowest available energy, that is, a tear will propagate along the shortest path through the weakest regions, thus minimizing the total failure energy. This mode of failure is illustrated in two dimensions in Figure 10, where a tear propagates from left to right. The dark circles represent the weaker material. Two potential pathways for tear propagation are illustrated: A and B. In the case of this illustration, the tear propagates the same distance, regardless of the path. However, by following path A, the tear propagates through a greater fraction of dark (lower strength) circles, thus minimizing the failure energy. It should be recognized that Figure 10 is for illustrative purposes only. In practice, the coa-

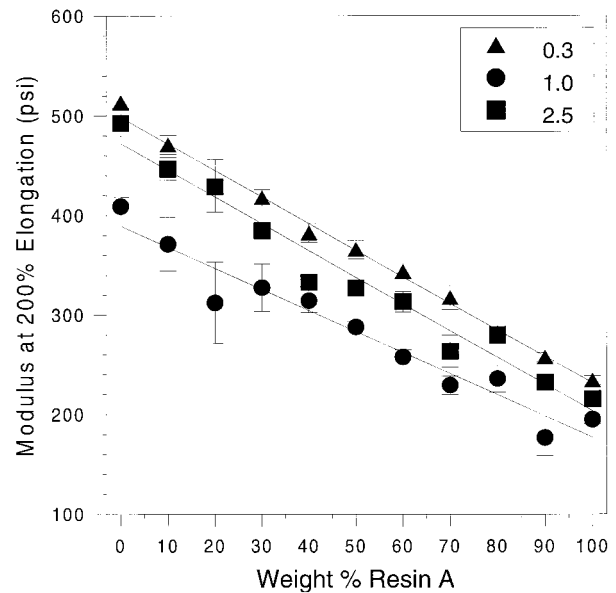


**Figure 9** Stress at 200% elongation as a function of blend ratio and particle-size ratio for blends of Resin A and Resin C.

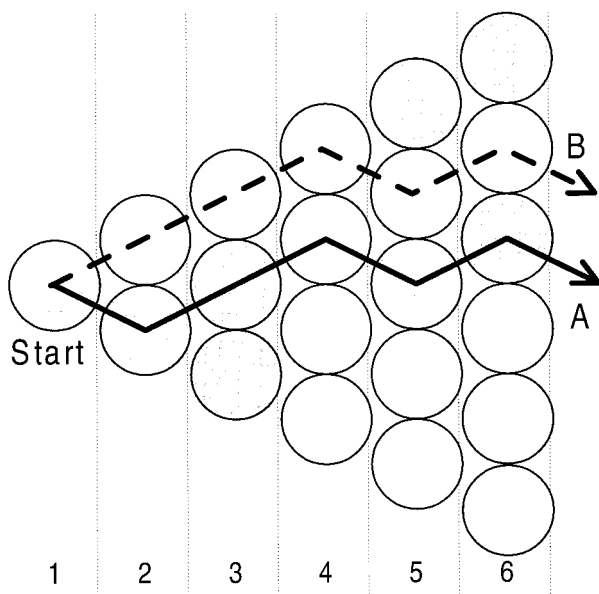


**Figure 10** Illustration of film failure scheme for Monte Carlo simulation.

lesced film would be void-free. It is assumed that microdomains of each constituent resin are preserved in the coalesced film, as discussed earlier.

Figure 10 illustrates that the tear propagation will be dependent on the film morphology, which is related to the particle diameter, the particle packing, and the blend ratio. It can be assumed that the particles will tend to pack randomly in a close-packed arrangement. Given all these assumptions, the packing and the tearing of blend films was modeled using a Monte Carlo simulation, using the representational method developed by Buldyrev.<sup>18</sup>

The Monte Carlo simulation can be described using Figure 10. From the starting particle, the tear can follow one of two potential paths, from layer one to two. The simulation dictates that when a choice of “weak” or “strong” particles is available the tear will always propagate through the weaker particle. When both particles are identical, a particle is chosen at random. These situations are shown in the transitions from layer two to three and from layer three to four. As the matrix is torn, the energy required to tear each particle is summed. Average failure energy for the matrix is calculated by dividing by total energy by the number of particles. Averaging multiple iterations on different randomly generated matrixes yields a simulated ultimate tensile strength. Using this modeling approach, there were no fundamental equations involved, only

sets of binary decisions followed by the calculation of an average.

Tensile failure was simulated in this fashion for three particle-size ratios. Filling of the matrix is difficult to program when unequally sized spherical particles are required. Therefore, in the interest of simplicity, large particles were simulated by using  $2 \times 2$  arrays instead of a single cell for a small particle as shown in Figure 11.

The visual output of the simulation is a valuable tool for understanding the film structure. Examples of three individual simulations are shown in Figure 12. Each image corresponds to a single random simulation. The soft phase (Resin A) is represented in black and corresponds to 20% of the total area in all cases. The dark line originating at the apex represents the failure path for the particular simulation. The two upper images in Figure 12 are for the cases where  $D_{\text{Resin C}}/D_{\text{Resin A}} \neq 1.0$ . When the particle-size ratio varies significantly from 1.0, there is a tendency for the particles to form a coarse, clustered morphology. In the case where the two particle types are of equal size, a fine structure results, as shown in the lower image of Figure 12.

The tensile strengths of blends of Resin C and Resin A were simulated. The tensile strengths of the neat Resin C and Resin A resins were specified as 2850 and 1200 psi, respectively. Twenty iterations were performed at each volume percent ratio. The modeling results are shown in Figure 13. The modeling results were fit to polynomials using nonlinear least squares. The results of the polynomial fits are tabulated in Table IV. Linear expressions fit the data reasonably well, but the quadratic fits are exceptional. The most compelling aspect of the curves is their similarity to the experimental tensile strength data shown in Figure 7. The simulated and experimental data follow the same quadratic functional form. The sim-

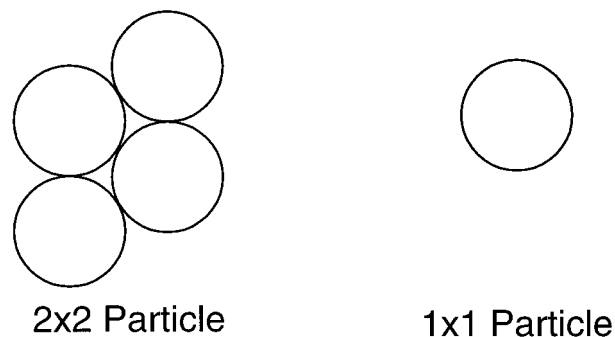


**Figure 11** Modeling particles.

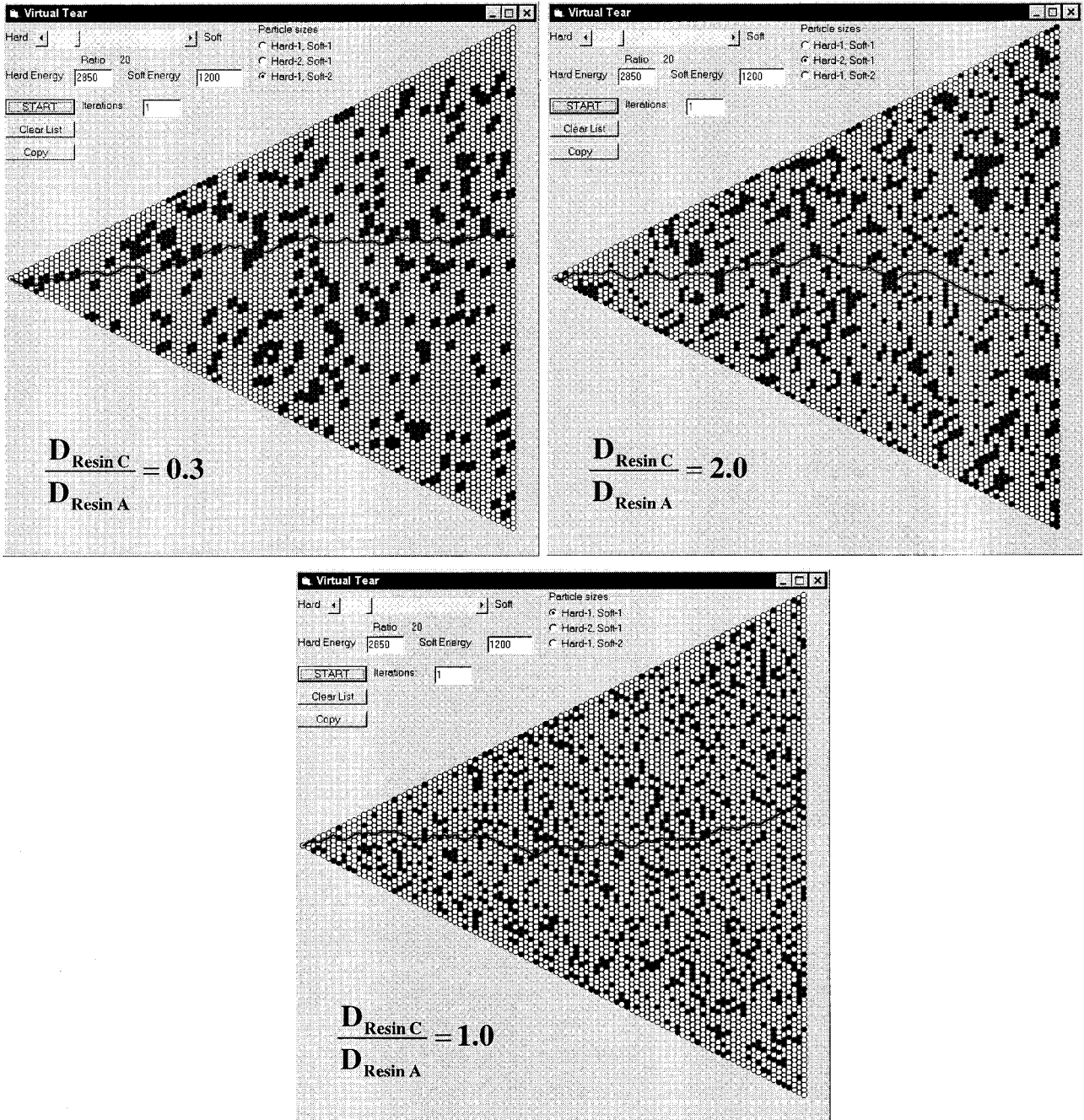


**Figure 12** Film morphology as a function of particle-size ratio (20% Resin A).

ulated data would not be expected to be identical to the experimental data, since the simulations were performed in two-dimensional space. In reality, the film is three-dimensional. In addition, many contributions to failure were ignored, including defects, microcracks, multiple cracks, and load distributions. Despite this, the agreement between the model and experimental data supports the assumption that the failure occurs by the lowest-energy path.

The simulation also provides information about the effect of the particle-size ratio on the tensile strength. The simulated tensile strength curves of the blends where the particle sizes are unequal ( $D_{\text{Resin C}}/D_{\text{Resin A}} = 0.5, 2.0$ ) are nearly identical. The curve for the equal particle size latexes has a lower  $x$  coefficient and a much lower  $x^2$  coefficient. This translates into a steeper slope at low Resin A concentrations and a flatter slope for high Resin A concentrations. The morphology

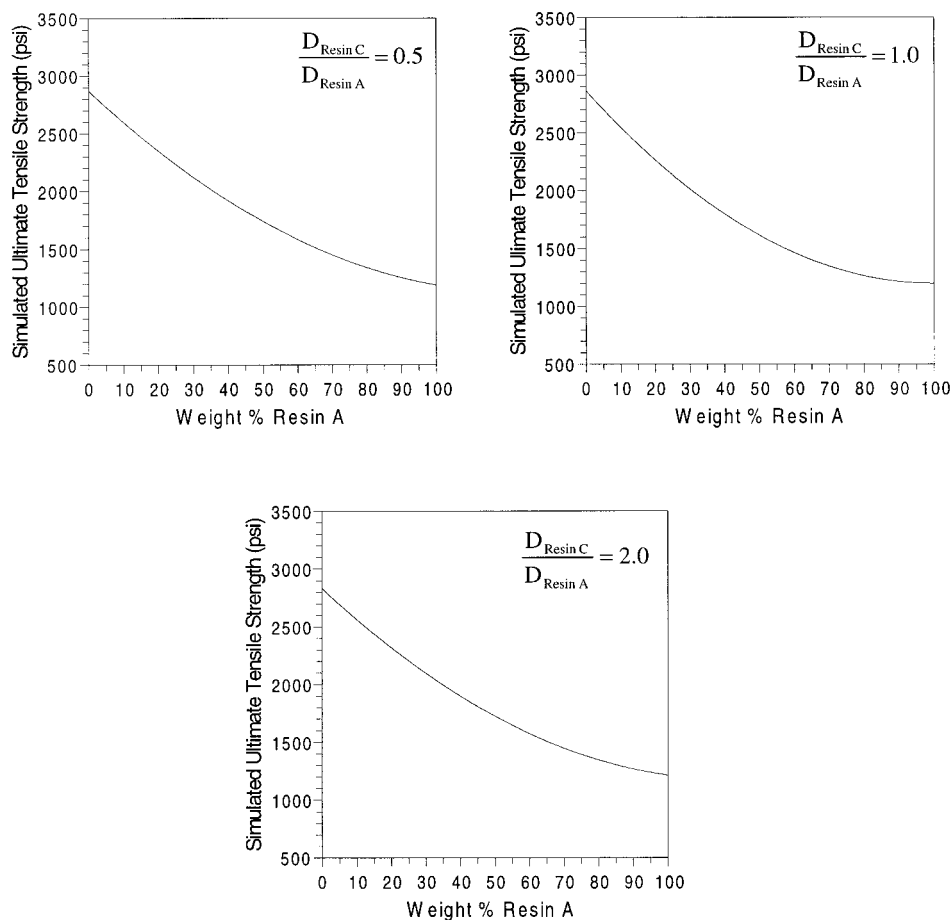


**Figure 13** Simulated ultimate tensile strength as a function of blend ratio for blends of Resin A and Resin C.

of the film has the most pronounced effect on the tensile strength when  $D_{Resin C}/D_{Resin A} = 1.0$ . There is an observable effect of particle size, according to the simulated data. However, the effect is subtle. From a practical perspective, variation of the particle-size ratio had a minor effect on the tensile properties. This is in contrast to the observations for latex coatings blends, where the particle-size ratio was found to have a dramatic effect on many properties. There are several differences in the nature of the two blend systems. An important contrast is that the hard particles in the

coatings blends remain discrete after the film formation.

## CONCLUSIONS

Polyolefin dispersions have many characteristics that make them potentially suitable for use in thin-film applications. The tensile properties of neat resins were measured. It was found that the neat resins did not have a desirable balance of tensile strength and softness (stress at low elon-

**Table IV** Polynomial Fit Results:  $a + bx + cx^2 = 0$

$D_{Resin C}/D_{Resin A}$	$a$	$b$	$c$	$R^2$ (Degree 1)	$R^2$ (Degree 2)
0.5	2870	-28.3	0.115	0.963	0.999
1.0	2863	-33.3	0.167	0.927	0.999
2.0	2832	-28.2	0.120	0.958	0.998

gation). Therefore, blend approaches were evaluated.

Dispersion blends refer to blends of two (or more) neat latexes. The effect of the blend ratio and the latex particle-size ratio was investigated for the dispersion blends, since these parameters are known to affect the film morphology. It was found that the blend ratio had a significant effect on the tensile performance. The tensile properties were independent of the particle-size ratio of the constituent dispersions. A quadratic functional relationship between a given tensile property and the blend ratio was found. Tensile failure of blend films was modeled using a Monte Carlo simulation, assuming that failure occurred via the lowest-energy pathway. The simulation generated similar quadratic relationships between the tensile strength and the blend ratio.

Blending of the polyolefin dispersions did not provide any performance advantages for thin-film applications. In fact, the blend film had properties that were inferior to the neat resin films. It would be of interest to investigate other elastomer emulsion or dispersion systems to determine if similar behavior is seen. The effect of crosslinking or vulcanization after film formation would also merit study.

Jeff Kosch designed and built the system used to make the dispersions evaluated in this study. John Oates finessed the process. Ken Reichel and Mike Lapham obtained the tensile performance data. Wendy Hoenig and Ron Hendershot initiated and supported the project. Ralph Czerepinski provided insight into particle packing and associated phenomena in latex blends.

## REFERENCES

1. Eckersley, S. T.; Helmer, B. J. *J Coat Tech* 1997, 69(864), 97.
2. Winnik, M. A.; Feng, J. *J Coat Tech* 1996, 68(852), 39.
3. Buckman, F.; Bakker, F. *Eur Polym J* 1995, 922.
4. Beckwith, M. C.; Najari, Z.; Hermes, E. *J Pharm Care Pain Sympt Control* 1994, 2(3), 25–36.
5. Pendle, T. D. *Plast Rubb Comp Process Appl* 1997, 26, 147.
6. (a) Lai, S. Y.; Wilson, J. R.; Knight, G. W.; Stevens, J. C. U.S. Patent 5 272 236 (to Dow Chemical Co.); (b) Lai, S. Y.; Wilson, J. R.; Knight, G. W.; Stevens, J.C. U.S. Patent 5 278 272 (to Dow Chemical Co.) Filed 1992, Issued 1994.
7. Hwang, Y. C.; Chum, S.; Guerra, R.; Sebanobish, S. In *ANTEC* 1994, p 3414.
8. Kusy, R. P. *J Appl Phys* 1978, 48, 5301.
9. Malliaris, A.; Turner, D. T. *J Appl Phys* 1971, 42, 614.
10. Floyd, F. L.; Holswort, R. M. *J Coat Tech* 1992, 64(806) 65.
11. Walther, B.; Bethea, J. U.S. Patent 5 574 091 (to Dow Chemical Co.) Filed 1992, Issued 1994.
12. ASTM D412–87; American Society for Testing Materials: Philadelphia, PA.
13. Eckersley, S. T.; Rudin, A. In *Film Formation in Waterborne Coatings*; Provder, T.; Winnik, M.; Urban, M., Eds.; ACS Symposium Series 648; American Chemical Society: Washington, DC, 1996; p 2.
14. Nishiuma, S.; Hasegawa, Y.; Miyazima, S. *Fractals* 1996, 4, 377.
15. Durham, S.; Lynch, J. D.; Padgett, W. J.; Horan, T. J.; Owen, W. J.; Surles, J. *J Compos Mater* 1997, 31, 1856.
16. Sahimik, M.; Arbabi, S. *Phys Rev B* 1993, 47, 713.
17. Murakami, I.; Fujiyama, K.; Okabe, N.; Yoshioka, Y. *Mech E. Conf Trans* 1996, 494, 251.
18. Buldyrev, S. *Directed Percolation*; Boston University Center for Polymer Studies; <http://polymer.bu.edu/~trunfio/java.tear.tear.html>; Dec. 4, 1997.